Nexus Network Journal (2026) 28:759–779
https://doi.org/10.1007/s00004-026-00874-y

NEXUS NETWORK JOURNAL
Architecture and Mathematics

RESEARCH

Algorithmic Design and Fabrication of Soft Curved-Folding

Duks Koschitz[1] · Riccardo Foschi[2] · Rupert Maleczek[3]

Received: 6 December 2025 / Accepted: 14 March 2026 / Published online: 16 April 2026

Abstract

This paper introduces an algorithmic method for designing and fabricating soft curved-folded surfaces using minimally stretchable thick panels, validated via the production of a free-form sculpture in fiber cement board. The proposed digital workflow combines crease-aware mesh generation with elastic simulation in Rhinoceros and Grasshopper. The study demonstrates how carefully calibrated constraints and real-time user adjustments enable the shaping of a complex, self-supporting form while minimizing material stretching and ensuring partial developability. A tailored manufacturing process, involving a digitally modeled and 3D-printed mold, facilitates the shaping of fiber cement with soft folds. Although tested on a 160 cm high sculpture, the method is broadly applicable to other foldable sheet goods with similar properties, offering the potential for both architectural and manufacturing applications.

Keywords Applied origami · Fiber cement board · Origami simulation · Curved creases · Mold Fabrication

Introduction

Curved folding has emerged as a key area in material-driven fabrication, enabling the creation of complex 3D shapes from flat sheets using digital workflows and advanced fabrication. While the differences between straight and curved folds are well studied, sharp versus soft folds have received less attention. Soft folding tech-

Duks Koschitz, Riccardo Foschi and Rupert Maleczek have contributed equally to this work

✉ Riccardo Foschi
riccardo.foschi@unibo.it

Duks Koschitz
duks@pratt.edu

Rupert Maleczek
Rupert.Maleczek@uibk.ac.at

1 School of Architecture, Pratt Institute, 200 Willoughby Str., Brooklyn, NY 11205, USA

2 Department of Architecture, Alma Mater Studiorum University of Bologna, Viale del Risorgimento 2, 40136 Bologna, Italy

3 Department of Design, i.sd, Faculty of Architecture, Technikerstrasse 21c, 6020 Innsbruck, Austria

niques broaden fabrication possibilities, allowing the use of flexible materials like thick textiles, leather, thin wood, or uncured fiber-reinforced concrete. This research aims to develop computational methods for generating and simulating soft folds from sharp fold lines, focusing on their applications and the interplay between geometry, material behavior, and fabrication.

Geometric Context

Although soft folding is a standard design method for textiles and is therefore described in available literature (Wolff 1996), a clear differentiation between straight and soft folding was first discussed in the context of the published work of Zhou et al. (Zhu et al. 2013). The simulation of textile behavior within different computational frameworks was explored in the 1990s, e.g., in Maya (Press 2009) or other platforms with their integrated mesh mass-spring models (Mozafary and Payvandy 2016). Mass-spring simulations are used in many design approaches in an architectural and/or structural context. In these cases, shapes are defined by an equilibrium of forces, e.g., in hanging chain models, which define their form via the manipulation of boundary conditions. Furthermore, tensile structures such as Minimal Surfaces and other textile techniques such as pleating, smokking, or tucking (Wolff 1996) can be simulated by 'mesh relaxation' (Senatore and Piker 2015).

Equilibrium configurations for cloth rely on material properties (e.g., stiffness) and boundary conditions (e.g., gravity, collisions), and origami designs similarly depend on material behavior and constraints such as mountain/valley assignments and folding forces. Folding patterns express these manipulations under calibrated parameters so the sheet does not tear or stretch, and numerous algorithms and software tools address straight and curved folds (Ghassaei et al. 2018; Mundilova et al. 2022; Tachi 2010; Suto et al. 2023; Lang 2012) have been developed for straight and curved folds.

These tools primarily target sharp creases, where adjacent surface patches meet with G0 continuity, and a dihedral angle is defined at every point along the fold line (Fig. 1). Sharp folds differ from soft folds (Zhu et al. 2013) that exhibit smooth transitions governed by the place the folding forces are applied and the stiffness of the material, turning a one-dimensional fold into a two-dimensional bent region that cannot be approximated by a single geometric line or curve.

Geometrically, a sharp fold could be regarded as a soft fold at the microscopic scale, yet in practice, they can be distinguished in sheet materials such as paper because sharp folds require plastic deformation or, in textiles, heat and/or moisture, leaving a clearly marked line or curve in the CP, whereas soft folds do not.

Measuring the dihedral angle of a soft fold requires tangents at both ends of the smooth folding zone rather than a single point on an idealized fold line, and soft folds are geometrically related to edge fillets (Pottmann et al. 2007) or mesh-subdivision (Zorin et al. 2000) with similar challenges at curved folds and high-degree vertices.

Soft folding enables folded designs (straight or curved) in elastic or stretchable materials, but its precise use within a smooth digital workflow requires defining key technical and computational parameters.

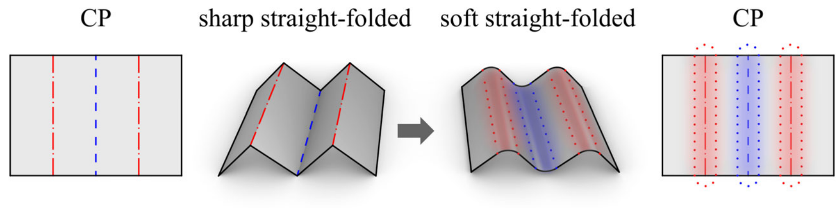

Fig. 1 Comparison between straight sharp creases (left) and straight soft creases (right)

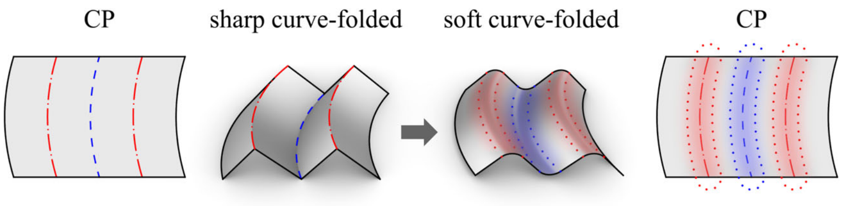

Fig. 2 Comparison between curved sharp creases (left) and curved soft creases (right)

The strategy presented here lets designers first work with sharp-folded CPs and later convert them to soft folds via elastic re-simulation, improving developability preservation compared to simple filleting.

Unlike Zhou et al. (Zhu et al. 2013), this method generates bespoke meshes around fold lines based on sheet thickness, target dihedral angle, and empirically measured material properties. It supports both straight (Fig. 1) and curved folds (Fig. 2).

Software Tools

Digital tools aimed at simulating the folding of developable surfaces exist, e.g., Origami Simulator (Ghassaei et al. 2018), Crane (Suto et al. 2023), Merlin (Liu and Paulino 2016; Paulino n.d.), Lotus (Mundilova et al. 2022), Freeform Origami, Rigid Origami Simulator, Origamizer (Tachi 2010). However, these applications are primarily optimized for rigid or sharp folding and do not address the requirements of soft folding.

A simple way to generate soft folds is to start from a sharply folded model and fillet the crease edges at the end, but this causes problems: filleting straight creases can create unrealistic shrinkage, and filleting curved creases can concentrate double curvature in small regions. A better approach is to re-simulate folding from the flat crease pattern, embedding controlled stretch, flexibility, and bending stiffness into a triangulated surface model that approximates curved geometry. This redistributes curvature over wider areas, reduces localized double curvature, and more accurately reflects the material's physical behavior.

The only known software specifically developed for soft folding is by Zhu, Igarashi, and Mitani (Zhu et al. 2013, n.d.). Although it has a solid theoretical foundation and is pioneering, it lacks integration with standard CAD tools used by architects and designers. It supports limited constraint types for shaping soft folds and does not offer crease-aware mesh generation.

Material Background

One particular focus of this investigation is the fabrication of soft folds with fiber cement boards. A short introduction to the material's history and its current fabrication methods is provided below. It is important to note that fiber cement boards serve as an exemplary case for sheet-based materials that can be deformed prior to curing into their rigid state.

Eternit fiber cement invented by Ludwig Hatschek in Austria around 1900, mixes Portland cement, water, and asbestos fibers for strong, lightweight, weather-resistant roofing panels (Ranachowski and Schabowicz, 2018, p. 1). His process uses a rotating cylinder to deposit slurry, enabling efficient thin, undulating panels; asbestos was later replaced by cellulose and polyvinyl alcohol fibers, matching original tensile and bending strength but with less flexibility in thicker panels. Designer Willy Guhl in 1954 created the 'Loop Chair' in collaboration with Eternit (now Swisspearl), and demonstrated the material's capacity to be bent when moist and formed into smooth, developable surfaces (Graur et al. 2023).

More recently, Grasser et al. reinterpreted and extended this approach by applying textile-inspired forming techniques to fiber cement. By utilizing gravity and friction (Maleczek et al. 2015), together with linear elements such as tubular rolls and stamps, they generated controlled folds and wrinkles with relatively small radii, supported by a cloth-simulation model. While this digital method was not used to design toward a specific target geometry, it successfully predicted the likely deformed shapes of fiber cement sheets using on the applied tooling.

Methodology and Workflow

The novel workflow presented in this paper capable of producing soft folded designs with minimally stretchable thick panels, including fiber cement boards, is structured in five different steps (Fig. 3):

1. preliminary exploration of shapes through manual folding experiments;
2. empirical evaluation of foldability using thick, wet cement boards;
3. development of an algorithmic tool for a soft-folding implementation;
4. design and fabrication of the mold;
5. validation of the proposed methodology through the fabrication of a soft-folded sculpture.

Advanced users can skip physical model exploration, as the proposed digital method offers sufficient versatility for direct virtual form-finding. The authors included an initial physical phase to honor designers' preference for tactile material interaction during ideation, and because paper models provided tangible validation and comparison against digital simulation results.

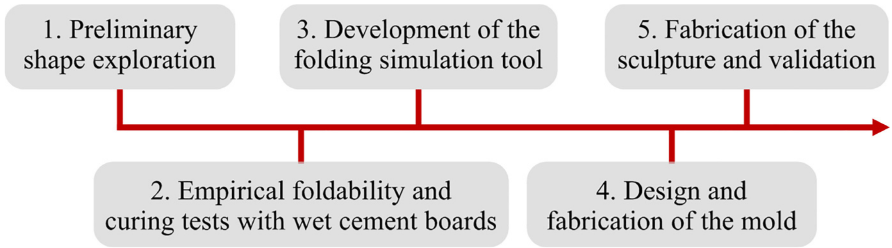

Fig. 3 Research steps

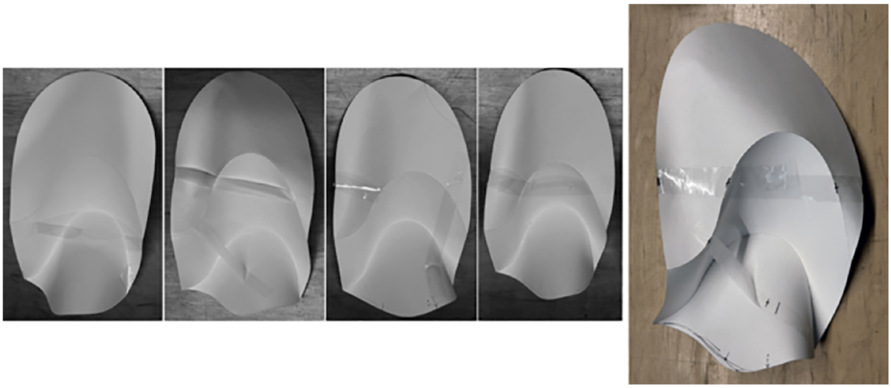

Fig. 4 Several examples of paper sketch models made with laser cutting. The shapes were held in place using tape. The color image of the final iteration on the right indicative tape anchor points are marked in black

Preliminary Shape Exploration

The case study presented in this article centers on an upright sculptural form featuring two primary creases: one mountain fold and one valley fold. To create a geometrically simple yet expressive configuration capable of demonstrating the design potential of soft folds, both creases were given an inflection point, resulting in an overall S-shaped curvature. The boundary geometry is derived from an oval outline. To explore the material and geometric behavior of the folds—specifically the achievable folding angles and surface curvature—numerous paper models were produced. Applying tape proved effective in constraining the paper into specific configurations during the exploration process. Determining the appropriate cutting plane to intersect the surface and generate the desired curvature along the ground plane required multiple iterative refinements (Fig. 4).

Marking the sketch models proved to be an effective method for documenting design modifications. It also served as a valuable tool for identifying the locations of potential tensile forces within the simulation. These areas were indicated directly on the models with pen or pencil and then connected using tape. Intersections with the ground plane were likewise recorded on the sketch models to support accurate spatial referencing (Fig. 4). The process of determining the final configuration involved scaling the paper

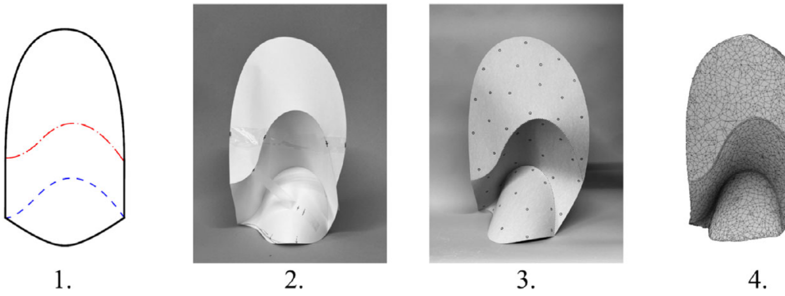

Fig. 5 (1) CP (mountain creases = red dash dotted, valley creases = blue dashed); (2) Sketch model held in place with tape to stabilize the shaping and to fix folding angles; (3) Refined model made with Vulcanex; (4) 3D-scanned mesh

Fig. 6 Preliminary folding tests of fiber cement boards displayed fractures and crimps in the areas around the sharp creases

sketch models to larger prototypes fabricated with Vulcanex, a cellulose-based board suitable for an increased scale. This larger prototype was subsequently 3D-scanned using positional reference dots to capture its precise geometry. The overall development sequence—from CP to paper model, to Vulcanex prototype, to scanned mesh—is illustrated in Fig. 5.

Empirical Testing of Wet Cement Boards

When the bending radius of a fiber cement board becomes too tight, the material is prone to tearing along the outer surface of the fold. This failure occurs because the fibers embedded in the cementitious matrix cannot stretch to accommodate the tensile strain induced during bending. The risk of tearing increases with material thickness, as the outer layers are subjected to greater elongation relative to the center axis of the sheet (Fig. 6). Empirical testing determined that the minimum safe radius allowing soft folding without tearing is approximately 30 mm for fiber cement sheets of 10 mm thickness.

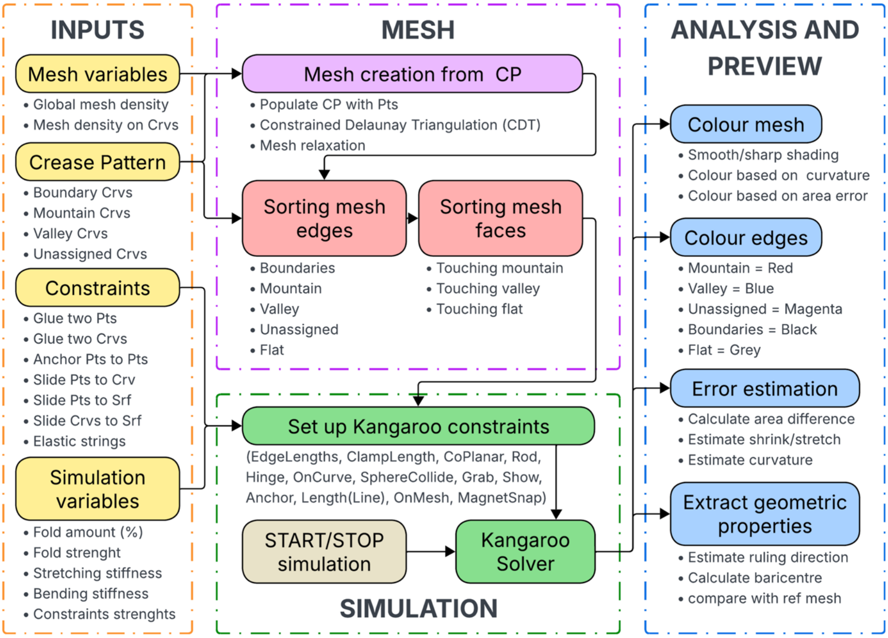

Fig. 7 Schematic Grasshopper flow

Development of the Folding Simulation Tool

The preliminary shape exploration is followed by the digital elastic simulation. This sequence allows designers to finalize the shape and subsequently convert it into its soft-folded counterpart. Rhinoceros (Mcneel 2025) and the visual programming language (VPL) Grasshopper (Rutten 2025), were used to achieve this task. The algorithm was designed for maximum user-friendliness and versatility, mimicking manual origami manipulation and physical constraints. The workflow comprises four main stages: (A) sharp-to-soft fold transformation; (B) crease-aware triangulated mesh generation; (C) constrained elastic folding simulation; (D) downstream analysis and visualization. A schematic of the Grasshopper algorithm appears in Fig. 7.

From Sharp Creases to Soft Folds

The transformation from sharp to soft folds (A) is done by manually offsetting the sharp crease curves of the initial crease pattern multiple times for finer control over each soft fold. During simulation, the fold angle is divided by the number of offsets to approximate a rounded edge. The offset distance x, given n offsets, is calculated as follows (notation in Fig. 8):

$$x = 2r \sin\left(\frac{\pi - \rho}{2n}\right); \tag{1}$$

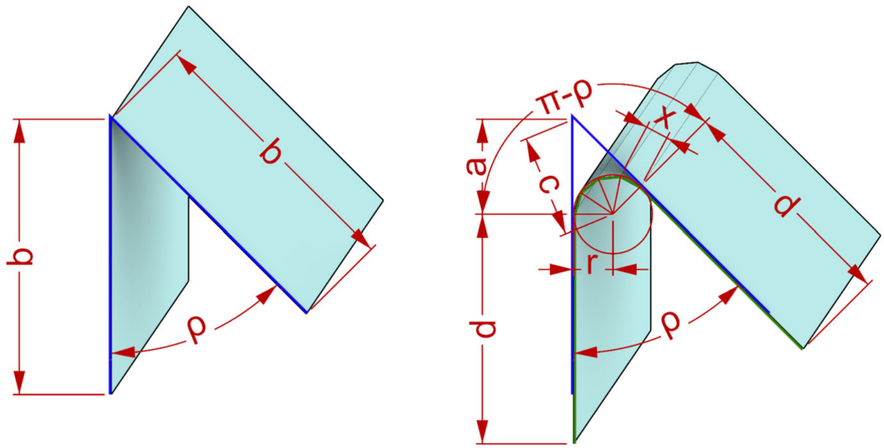

Fig. 8 Notation for the formulations enabling the conversion from sharp to soft creases. The blue line is the section of the sharp creased surface, and the green line is the section of the surface after softening. Note that the green line slides slightly to accommodate the length of the rounded section in order to preserve the same total length

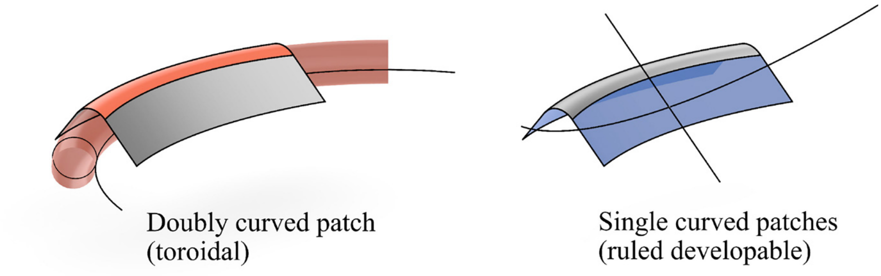

Fig. 9 For illustrative purposes, a soft-curved crease can be represented as a doubly curved toroidal patch, while the adjacent surfaces as singly curved developable patches. In physical models, however, this behavior is not typically observed because the doubly curved surface area also expands on the adjacent surface patches and is not uniformly arranged as in the image

$$a = r \cot \frac{\rho}{2}; \tag{2}$$

$$d = b - \frac{1}{2}nx. \tag{3}$$

Where: x denotes the offset distance from the sharp crease; ρ represents the maximum fold angle; n is the number of offsets, predetermined by the user according to the desired level of discretization; a indicates the distance between the center of the soft fold and the original sharp corner; b is the original length of the adjacent face section, and d corresponds to the reduced length of the same face after conversion from sharp to soft folding.

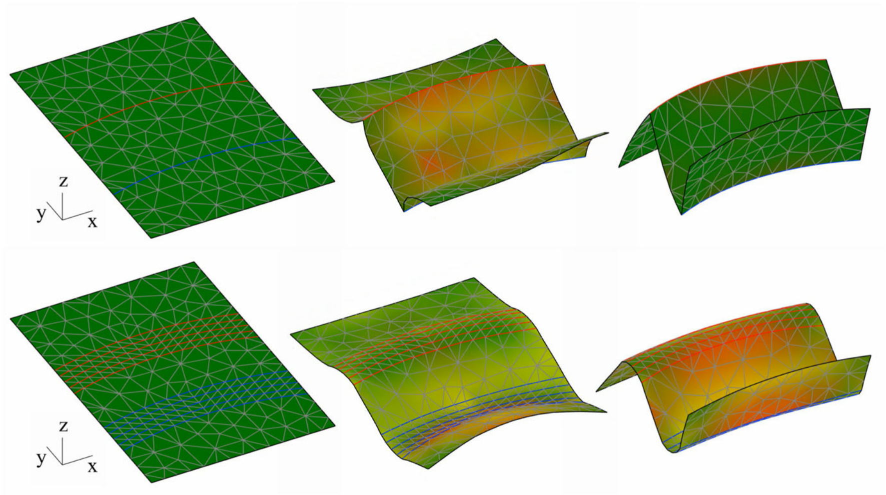

Fig. 10 Soft folding of curved creases always results in doubly curved surfaces (non-developable), while sharp curved creases result in single curved developable surfaces (developable). Green indicates no deformation, red denotes compressive strain, and yellow represents tensile strain

In general, when curved creases are softened, the resulting surface necessarily becomes doubly curved and non-developable, as the soft creases approximate toroidal patches (Fig. 9). This geometry implies a degree of in-plane stretching within the material—an inherent property of wet fiber cement. Based on the empirical testing, the minimum safe radius allowing soft folding without tearing is approximately 30 mm for fiber cement sheets of 10 mm thickness. Because the fold angle may vary along a curved crease (Tachi and Epps 2011), the corresponding offsets that determine the softened crease width also would vary. Although the proposed method is, in principle, capable of producing variable-radius soft creases, in this study, for design consistency, we apply uniform soft-fold offsets across all folds in the pattern. Consequently, the minimum soft-fold radius is estimated at the point on the crease where the maximum fold angle occurs. Why a sharp-creased preliminary model is not simply softened after folding by beveling or filleting, rather than re-simulating a surface with soft folds embedded directly in its CP, can be explained by two main reasons. First, beveling sharp creases causes material loss, which can lead to unexpected issues during fabrication. Second, converting sharp creases into soft ones afterward confines doubly curved regions to the beveled patches. By contrast, re-simulating the pattern with soft creases from the start distributes doubly curved areas across adjacent faces, reducing localized material stresses which better reproduce the observed physical properties of the concrete panel in use (Fig. 10).

Crease-Aware Triangulated Mesh Generation from a CP

The mesh generation (B) consists of the following 6-step procedure (Fig. 11):

1. draw the sharp-creased pattern;

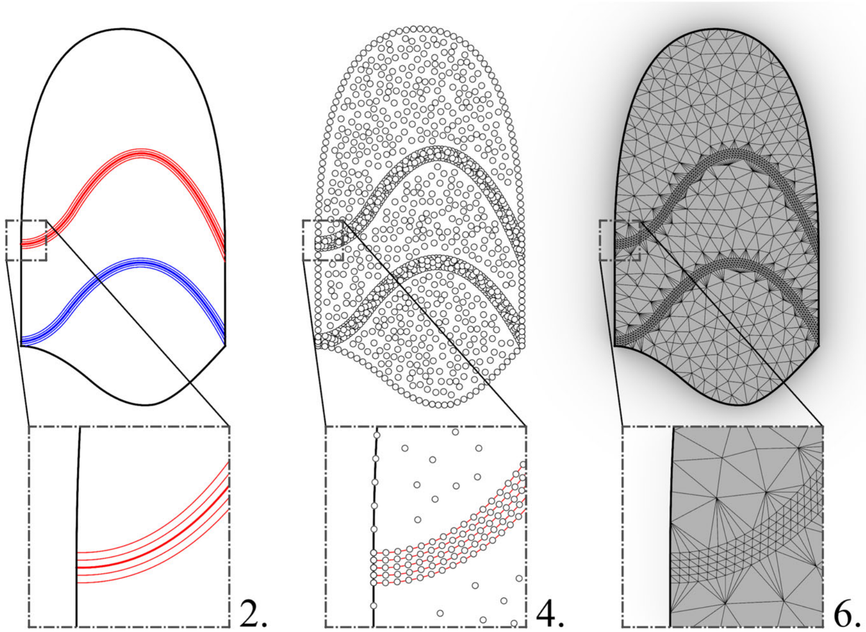

Fig. 11 Core steps for crease-aware mesh generation

2. convert sharp to soft creases by offsetting them;
3. populate the CP with points;
4. populate creases and boundaries with points;
5. mesh generation through Constrained Delaunay Triangulation (CDT);
6. constrained mesh relaxation.

In step 1, the CP is drawn as curves on the xy plane and converted into its soft folded counterpart in step 2 according to the method explained in section 2.3. In step 3, a prescribed number of random points are uniformly distributed within the boundaries; to improve the quality of the Delaunay triangulation, all points located within a threshold distance from the edges and creases are removed. In step 4, points along the creases are positioned such that their spacing corresponds to the average distance between neighboring points in the initial point cloud. An input slider is provided to allow the user to adjust point spacing both on the creases and in between. In step 5, since the native Grasshopper Delaunay triangulation (Pottmann et al., 2015, p. 617) component does not support point and edge constraints, a custom C# node was scripted to access the 'CreateFromTessellation' native Rhino API method (Rhino API https://developer.rhino3d.com/api/rhinocommon/rhino.geometry.mesh/createfromtessellation), which allows the actuation of a constrained Delaunay triangulation (CDT) (Chew 1987). This method also keeps the mesh borders consistent in case of concave borders and meshes with holes. The simple scripted node uses two lists of edges and points (respectively x and y) and outputs a CDT mesh with the following simple code:

```
private void RunScript(List<Point3d> x, List<Polyline> y,
```

```
 ref object A)
{
A = Mesh.CreateFromTessellation(x, y, Plane.WorldXY, false);
}
```

It must be noted that, to avoid errors during the generation of the mesh, the x y input lists must not have duplicated geometries. Finally, in order to improve triangle regularity and their even distribution, the generated mesh is refined with a constrained relaxation algorithm (Tedeschi, 2014, p. 374) using the Kangaroo plugin. The constraints consist of all the points located along creases and boundaries, which ensures that the discretization remains uniform and consistent with the initial CP in the presence of curved features. The input parameters are configured such that the mesh becomes locally denser in the proximity of soft creases, corresponding to regions of higher curvature in the folded model. The mesh density must be carefully balanced, not excessively coarse nor overly refined, in order to maintain both accuracy and computational efficiency (Fig. 11).

Constrained Elastic Folding Simulation

The third step (C) consists of actuating a constrained elastic simulation (Song et al. 2024) by applying forces to the mesh. Iterative elastic simulations in Grasshopper can be carried out using the Kangaroo2 plugin (Piker n.d.), which has been natively integrated into Rhinoceros in version 8 (Mcneel 2025).

All edges of the mesh are categorized and assigned as mountain, valley, unassigned, or facet creases. Mountain and valley creases are defined as oppositely oriented; unassigned creases are set to remain loose during motion (they are not used in this case), whereas facet creases are constrained to remain flat (i.e., a dihedral angle between adjacent facets equal to π), although some compliance will appear in the simulation, allowing the facet creases to bend slightly. This terminology is consistent with the one used in Origami Simulator (Ghassaei et al. 2018).

To classify the mesh edges as mountain, valley, unassigned, or facet creases in Kangaroo, the 'HingePoints' utility node and the 'Hinge' Goal node were used. Each mesh edge was categorized based on its proximity to the corresponding input curve retrieved from the input CP (Fig. 12).

Folding forces defined by the operator through Kangaroo's Goal Nodes are applied to all mesh edges according to their classification. Forces acting on facet creases (all those mesh edges which are not unassigned, mountain, or valley) approximate the material's bending stiffness, while additional forces regulate the surface's stretching stiffness (e.g., EdgeLengths, Hinge). Further geometric constraints, such as anchor points, attractor planes, rail curves, elastic wires, and collisions, were also simulated using a series of Kangaroo Goal Nodes (e.g., EdgeLengths, ClampLenghts, CoPlanar, OnMesh, OnCurve, SphereCollide). It must be noted that a custom C# Hinge component was developed by Daniel Piker (Piker 2019) to address a known limitation of Kangaroo's native Hinge component, which tends to introduce an unexpected increase in energy when the fold angle approaches π. These constraints, used simultaneously, replicate the forces applied manually to the physical mock-up, thereby enabling the mesh to fold into its intended shape.

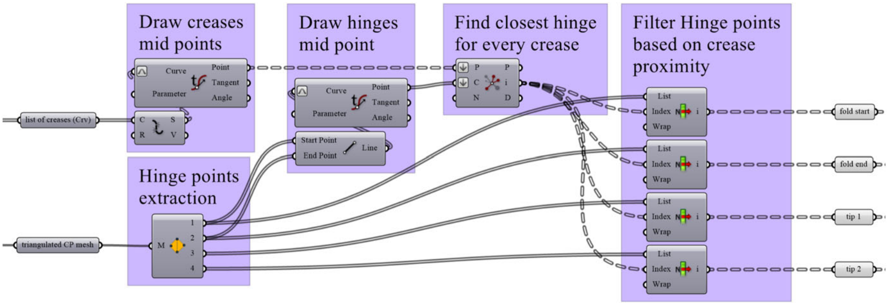

Fig. 12 Grasshopper node cluster for filtering hinges based on mountain valley assignment, extracted from the Grasshopper VPL script

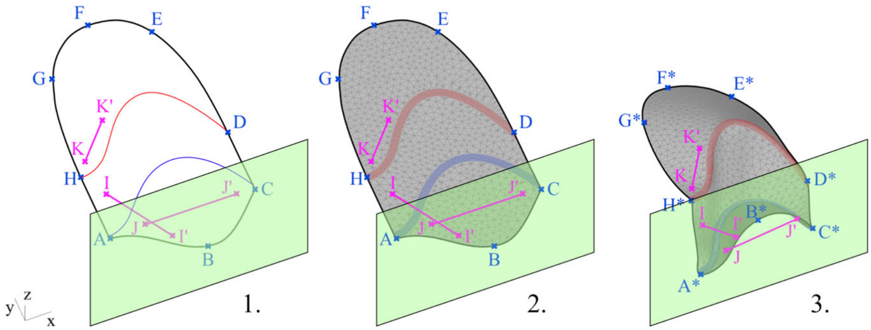

Fig. 13 Soft-curved-folding simulation. (1) CP and constraints are drawn as curves and points; (2) the mesh is generated automatically; (3) the simulation is run and the following constraints are applied: the faces adjacent to valley and mountain creases rotate with respect to the relative hinge edge, ABCDEFGH points are attracted to specific target anchor points, I-I' J-J' K-K' lines behave like elastic bands glued to specific uv points on the surface, the curve passing through points ABC tend to be coplanar with the green plane, all the other faces of the mesh try to stay coplanar to their relative adjacent faces to simulate bending stiffness

During simulation, the mesh dynamically responds to the applied constraints, and users can adjust parameters interactively in real time until the desired configuration is achieved (Figs. 13, 14).

Figure 13 displays the unavoidable deformations appearing near the soft folds; however, these deformations remain minimal (less than $\pm 1.1\%$ area error), as the ability of the simulation to distribute strain over adjacent mesh areas limits the impact of local errors.

The 3D-scanned mesh of the Vulcanex final model served as the reference surface, with constraints tuned until the simulated mesh closely matched it. Exact matching was neither expected nor possible, since Vulcanex creases are sharp while simulated ones are soft. Eight boundary anchor points loosely guided the mesh toward the scan (Fig. 15); oversampling was avoided to prevent intrinsic sharp/soft differences from amplifying errors.

Once all the constraints are set up, the Kangaroo solver reads the input GoalNodes and iteratively minimizes the total sum of the weighted squares of all the displacement vectors set by them, by following this rule:

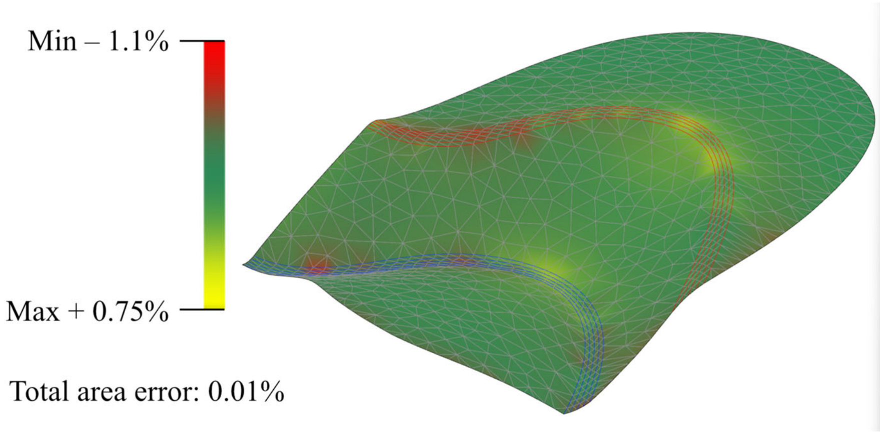

Fig. 14 Developability error due to the double curvature introduced by the soft creases. Face area error range is between −1.10% to +0.75%

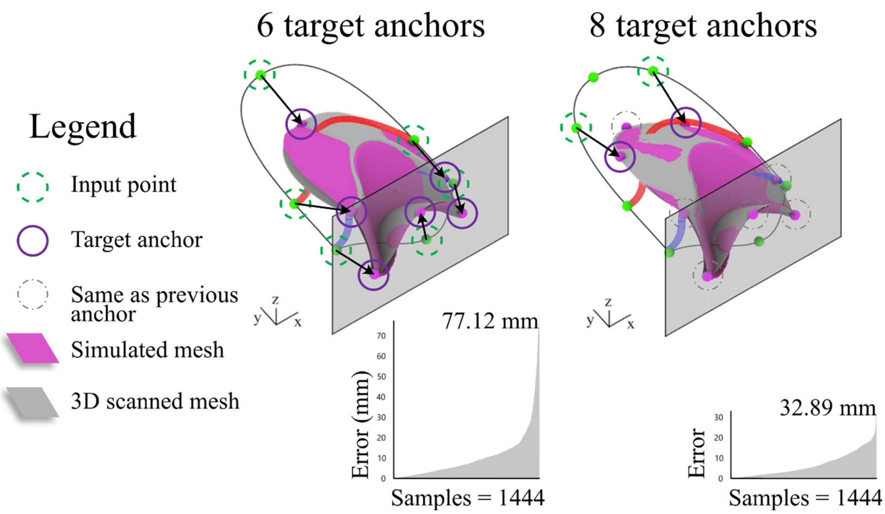

Fig. 15 Variable accuracy between simulated and scanned meshes based on the number of anchor points

$$\mathbf{P}_{i,\text{new}} = \mathbf{P}_{i,\text{cur}} + \frac{\sum_{j=1}^{n} \omega_j \cdot \mathbf{G}_j}{\sum_{j=1}^{n} \omega_j}, \tag{4}$$

where: i denotes the vertex/particle $\mathbf{P}$, n the number of goals acting on that vertex/particle, ω the weighting assigned via Grasshopper's nodes, and $\mathbf{G}$ the displacement vector exerted by the constraint/GoalNode j (Brandt-Olsen, 2016, P. 27). This formulation ensures that the simulation converges toward an equilibrium state. Digital simulation allows advanced users to bypass the preliminary stages of making physical sketch models and 3D-scanning, which results in a more sustainable and cost-efficient design process.

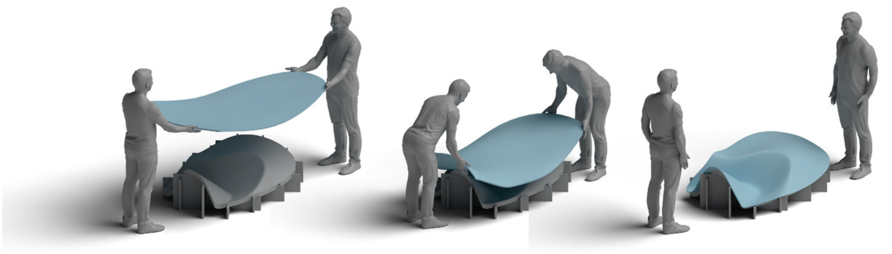

Fig. 16 Two people placing the wet cement board. The board is then trimmed and polished on the edges after it dries

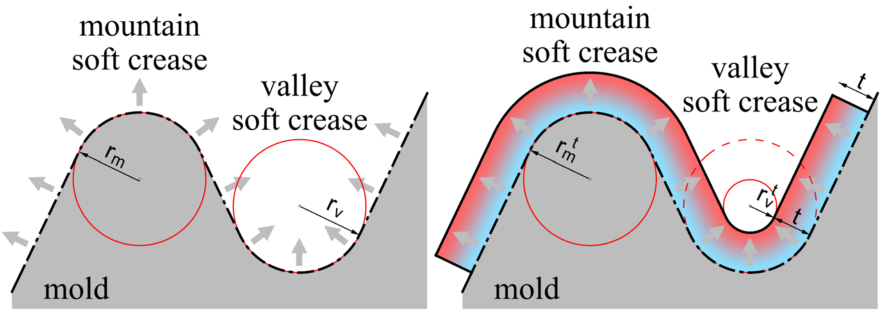

Fig. 17 Addressing soft fold radii considering thickness

Design and Fabrication

To facilitate the curing of the wet cement board while preserving its intended geometry, a full-scale (1:1) mold was fabricated. Unlike conventional formwork used for liquid cement casting, this process requires only a single-sided mold, on which the malleable cement board is manually placed and left to set for several hours to achieve reasonable stability (Fig. 16).

Fabrication-Constrained Thickening

If the mold uses the simulated zero-thickness surface as the top interface, this same surface forms the bottom interface of the wet cement board. Consequently, the board's thickness accumulates above this interface, causing the top and bottom surfaces of a mountain or valley soft crease to have different radii due to material thickness (Fig. 17). To avoid unexpected results, thickness and a safe radius for soft folds must be considered early in the design process.

When the thickness is accumulated on the same side of the zero-thickness surface, transforming a surface with prescribed soft fold radii for mountain (r_m) and valley (r_v) folds, into its thickened version with thickness t, the resulting effective mountain (r_m^t) and valley (r_v^t) fold radii can be expressed by the following equations:

$$r_m^t = r_m, \tag{5}$$

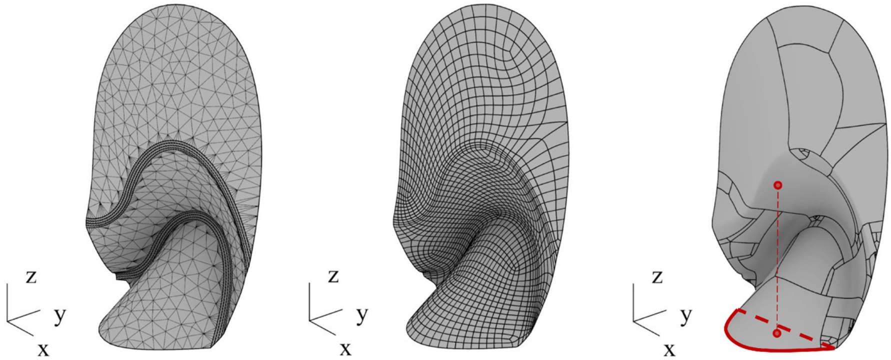

Fig. 18 Conversion from triangulated mesh, to subD, to NURBS polysurface. The Barycenter analysis is represented in Red

$$r_v^t = r_v - t, \tag{6}$$

The mold is fabricated by designing its top interface surface. If both valley and mountain soft creases are designed with identical radii, the thickness will cause the corresponding radius on the opposite interface surface to increase or decrease. To achieve consistent radii between mountain and valley creases, the radii must therefore be calculated differently for each case, accounting for both thickness and fold angle on a point-by-point basis.

While this approach is feasible, it is computationally demanding because it requires relating the soft fold radius to the effective simulated fold angle at each crease point. To reduce complexity, we estimated the maximum fold angle across the entire CP and used this value to calculate a global soft fold radius, which was then adjusted based on the expected material thickness. This radius was then uniformly applied to all soft creases, avoiding the need for point-by-point adjustments. This strategy was sufficient for our purposes, as the primary goal was to ensure a minimum soft fold radius large enough to prevent crumpling and cracking of the material, but small enough to give the impression of sharp folds from a distance. It must be noted that any change in thickness due to stretching and compression of the material was considered negligible in this case.

Mesh to NURBS Conversion

The simulated mesh was triangulated to minimize shear and preserve developability during simulation, but this faceting is unsuitable for high-quality molds. Thus, it is converted to a smooth NURBS surface via: baking to Rhino, rebuilding as a quad mesh with QuadRemesh, interpolating to a SubD surface (McNeel 2025), and converting to NURBS polysurface. This smooth polysurface supports standard NURBS workflows like offsetting for solids and Boolean operations for fabrication. Before fabrication, the surface barycenter was tested to project within the base's convex boundary to ensure stability (Fig. 18).

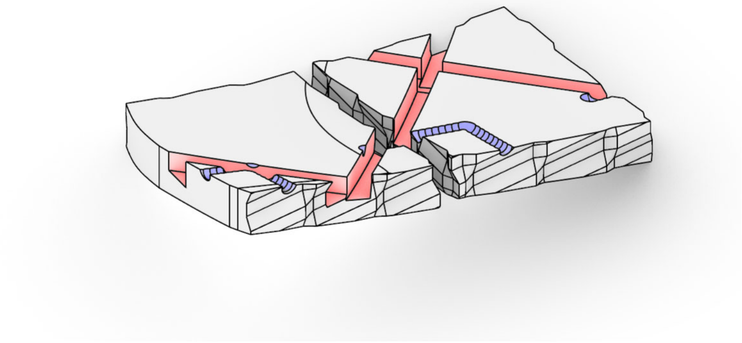

Fig. 19 Bottom view of two 3D-printed parts assembled. The grooves that align with the wooden frame are marked in red, and the round engravings for orienting the parts are marked in blue

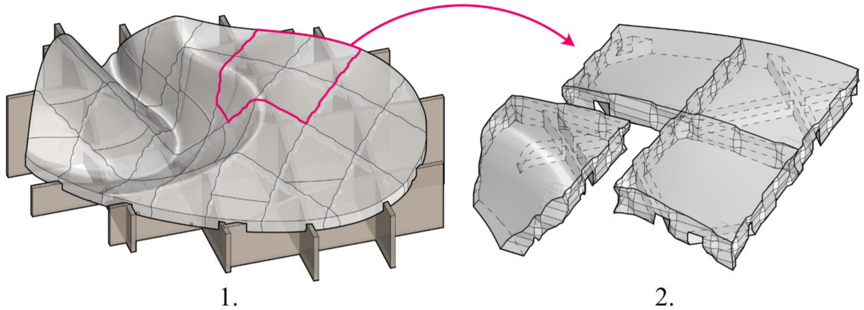

Fig. 20 (1) Assembled mold on a wooden frame; (2) four modules prepared for 3D printing

Assembly of the Mold and Sculpture

The mold was fabricated using 3D-printed parts made from recycled PLA (rPLA), mounted on a wooden substructure arranged as a rectangular grid. After use, the PLA material will be recycled into new rPLA filament. Because of the printer's build-volume constraints, the digital model was subdivided into segments that would fit within the used 3D-Printer (Bambu Lab 2023). The 3D model was extruded 50 mm along the Z-axis to create sufficient volume for structural stability and further processing. A square grid with 221 mm edges, projected in the Z-direction, defined the subdivision pattern. This grid, combined with embossed part markings, enabled a self-aligning, puzzle-like assembly system for efficient construction (Fig. 19). The 260 mm waffle grid was rotated 45° relative to the main grid to reduce wood use and milling time, and milled from 19 mm OSB boards on a 3-axis CNC mill (Fig. 20).

The one-sided mold assembly involved several steps. First, all parts were 3D-printed, then sanded and loosely placed on the wooden waffle structure, where friction provided initial rigidity. Once fitted, parts were glued; remaining joint gaps were filled and smoothed with epoxy filler for a seamless surface on the fiber cement board. The mold was transported to the Swisspearl factory, where wet fiber cement was laid on

Fig. 21 (1) 3D-printed mold assembled and filled with epoxy filler on a wooden waffle structure; (2) wet fiber cement board on the mold; (3) self-supporting sculpture after curing

it (Fig. 21). Full curing took 23 days, but structural stability occurred after about 10 h; the self-supporting sculpture shows no wobble.

Discussion and Future Work

This research presents a computational method that enables controlled folding behavior while accommodating specific material constraints. By incorporating user-defined parameters within the constraint system, the approach balances automation with designer agency, a critical feature for intentional form generation rather than purely algorithmic form-finding.

The presented workflow and implementation proved to be a versatile and valid tool for designing smooth folded designs. However, it suffers from reduced performance in the case of complex CPs, which require dense meshes and self-collisions, due to Grasshopper's known inability to GPU-parallelize all processes. The tool can be improved in terms of UI, and bending behaviors are simulated only qualitatively without aiming to reproduce exact material properties. This is a non-trivial, interesting topic for future research.

The elastic simulation does not aim to represent the material behavior in detail (e.g., time-dependent curing, heterogeneous elastic modulus, fiber direction), but it is only used as a means to arrive at an equilibrium configuration for the geometric definition of the shape. More in-depth material simulation would require a different investigation method, software, and hardware, which could be studied in future work.

Future work will also focus on the change and adaptation of folding angles along soft creases, and its potential to generate sharp creases that will transition to soft creases along a single spatial curve, exploring the relation and boundaries between soft and sharp folds. An ongoing work includes the development of the logic to differentiate input fold angles per crease.

The evaluation phase emphasized qualitative assessment, without systematic benchmarking of geometric accuracy, dimensional tolerances, or structural failure thresholds. Establishing quantitative validation metrics could be an important direction for future work. Regarding fabrication, the current workflow relies on manual draping and handling, which inherently limits repeatability and scalability. However, the method's framework is adaptable and could be extended to machine-guided procedures in future implementations.

Conclusion and Contributions

The presented method requires a 2D CP and a series of constraints that define the forces that shape the surface while preserving developability as much as possible. The user can tweak these inputs in real time to reach the desired shape. The simulation-based workflow allows for an exploration of the shaping as well as the construction of a mold for fabrication. The novel algorithm-aided method presented here enables the design and fabrication of soft curved folded surfaces.

Regarding the algorithm, several aspects can be highlighted. The developed method of mesh generation is crease-aware in its alignment with the initial CP. The soft fold area in the presented method is interpreted and represented as an offset region with variable resolution, which is different from previous software approaches. The soft fold radius can be adjusted in a uniform or non-uniform way along the soft fold to user and/or material-specific requirements. The presented method has been implemented and well integrated into a widely used, commercially available CAD software for designers. The tool can thereby reach wider audiences in a variety of design contexts. The presented tools and their simulation capabilities are highly versatile and can accommodate many different constraints for specific use cases. This allows for ease of customization of the tool itself. The presented case study consists of a 160 cm sculpture made by folding wet fiber cement boards. This physical experiment serves to validate the proposed method and also tests its application at a large scale. The workflow for the proposed fabrication can be applied to other foldable materials with similar properties for other applications in the architectural or manufacturing fields.

Acknowledgements We express our gratitude to the participants of the Structural Origami Gatherings, whose direct and indirect contributions promoted critical thinking and nurtured a vibrant international multidisciplinary research community, without which the network that made this paper possible would never have come into being. Beate Diem and Markus Plackholm at Swisspearl have been instrumental in supporting this project. Ernest Hager and Rupert Assanger at the University of Innsbruck helped with the 3d printing and mold making. We also thank Daniel Piker, who helped develop the custom Hinge Node for Kangaroo.

Author Contributions All authors contributed equally to this work and have read and agreed to the published version of the manuscript.

Funding Open access funding provided by Alma Mater Studiorum - Università di Bologna within the CRUI-CARE Agreement. This research was supported primarily by Duks Koschitz's personal funds, with additional support from the University of Innsbruck and from RFO funds of Bologna University. The Mold Fabrication was supported by Rupert Assanger from the WAU. Büro für gepflegte Gestaltung, and Ernest Hager from the Architectural model shop at the University of Innsbruck. The fiber cement material was sponsored by Swisspearl.

Data Availability Statement The code presented in this article is available on GitHub at the following link: https://github.com/Riccardo-Foschi/GrasshopperOrigami-Simulator-Kangaroo.

Declarations

Conflict of Interest The authors declare that there is no conflict of interest.

Ethics Approval and Consent to Participate Not applicable.

Consent for Publication Not applicable.

References

Bambu Lab 2023. Bambu lab x1 carbon 3d printer. https://www.bambulab.com/en/x1-carbon. Used in this study for 3D printing of experimental components

Brandt-Olsen, C.S. 2016. Calibrated modelling of form-active structures The Technical University of Denmark.

Chew, L.P. 1987. Constrained delaunay triangulations. Proceedings of the third annual symposium on computational geometry (pp. 215–222).

Ghassaei, A., Demaine, E.D., Gershenfeld, N. 2018. Fast, interactive origami simulation using gpu computation. Origami7:1151–1166,

Graur, A.M., Patachi, L., OPRICA, A.M. 2023 Geometric study in the realization of concrete furniture. Journal of Industrial Design and Engineering Graphics18217–22,

Lang, R.J. 2012 Origami design secrets: mathematical methods for an ancient art. CRC Press.

Liu, K., Paulino, G.H. 2016 Merlin: A matlab implementation to capture highly nonlinear behavior of non-rigid origami. Proceedings of IASS annual symposia (Vol 2016, pp. 1–10).

Maleczek, R., Grasser, G., Filz, G.H., Ladinig, J. 2015 Self-organized folding with gravity and friction as guiding concept. P. Wang-Iverson, R.J. Lang, M. Yim (eds), Origami 6: Sixth international meeting of origami science, mathematics, and education (p. 138). Providence, RIAmerican Mathematical Society.

McNeel 2025 subdobject. https://developer.rhino3d.com/api/rhinocommon/rhino.docobjects.subdobject. Used in this study as a step to generate a NURBS Surface

Mozafary, V., Payvandy, P. 2016 Study and comparison techniques in fabric simulation using mass spring model. International Journal of Clothing Science and Technology285634–689,

Mundilova, K. , Demaine, E. , Foschi, R. , Kraft, R. , Maleczek, R. , Tachi, T. 2022 Lotus: A curved folding design tool for grasshopper. Acadia 2021 realignments: Toward critical computation: Proceedings of the 41st annual conference of the association for computer aided design in architecture (pp. 194–203).

Paulino, G.H. Paulino software. software. https://paulino.princeton.edu/software.html

Piker, D. Kangaroo. https://grasshopperdocs.com/addons/kangaroo-2.html Online; accessed 30-September-2025

Piker, D. 2019 Rhinoceros forums: Rest angle behaviour in hinge component. https://discourse.mcneel.com/t/rest-angle-behaviour-in-hinge-component/90999/2

Pottmann, H. , Asperl, A. , Hofer, M., Kilian, A. 2007 Architectural geometry. Bentley Institute Press.

Pottmann, H. , Eigensatz, M. , Vaxman, A., Wallner, J. 2015 Architectural geometry. Computers & graphics47145–164,

Press, A.M. The learning maya 2009 collection: Foundation, modeling & animation, and special effects. John Wiley & Sons. Includes DVD and covers the full Maya 2009 pipeline.

Ranachowski, Z., Schabowicz, K. 2018. The fabrication, testing and application of fibre cement boards. Newcastle upon Tyne, UKCambridge Scholars Publishing.

Rhino API CreateFromTessellation method. RhinoCommon API documentation. https://developer.rhino3d.com/api/rhinocommon/rhino.geometry.mesh/createfromtessellation

Robert McNeel & Associates 2025 Rhinoceros (version 8). https://www.rhino3d.com/it/ Online; accessed 30 September 2025

Rutten, D. Grasshopper. https://www.grasshopper3d.com/ Online; accessed 30-September-2025

Senatore, G., Piker, D. 2015 Interactive real-time physics -an intuitive approach to form-finding and structural analysis for design and education. Computer-Aided Design6132–41, https://doi.org/10.1016/j.cad.2014.02.007

Song, K. , Li, H. , Li, Y. , Ma, J., Zhou, X. 2024 A review of curved crease origami: design, analysis, and applications. Frontiers in Physics121393435,

Suto, K. , Noma, Y. , Tanimichi, K. , Narumi, K., Tachi, T. 2023 Crane: an integrated computational design platform for functional, foldable, and fabricable origami products. ACM Transactions on Computer-Human Interaction3041–29,

Tachi, T. 2010 Tachi software.

Tachi, T., Epps, G. 2011 Designing one-dof mechanisms for architecture by rationalizing curved folding. International symposium on algorithmic design for architecture and urban design (algode-aij). tokyo (Vol 5, p 6).

Tedeschi, A. 2014. Aad algorithms-aided design: Parametric strategies using grasshopper. BrienzaLe Penseur Edizioni.

Wolff, C. 1996. The art of manipulating fabric / colette wolff. Iola, WisKrause Publications.

Zhu, L., Igarashi, T., Mitani, J. Soft folding software. https://www.jst.go.jp/erato/igarashi/en/projects/SoftFolding/index.html

Zhu, L. , Igarashi, T., Mitani, J. 2013October. Soft folding. Proceedings of the 21st pacific conference on computer graphics and applications (pacific graphics 2013) (Vol 32). SingaporeComputer Graphics Forum. Held October 7–9, 2013

Zorin, D. , Schröder, P. , DeRose, T. , Kobbelt, L. , Levin, A., Sweldens, W. 2000 Subdivision for modeling and animation. SIGGRAPH 2000 Course Notes.

Duks Koschitz PhD, is a Professor of Design & Technology at Pratt Institute since 2013 where he teaches undergraduate and graduate courses. He is the Director of the d.r.a. (center for design research at Pratt), a research laboratory that investigates 2d manufacturing processes that can be linked to specific topics in computational geometry. In 2015 Duks completed his dissertation at M.I.T. on the Curved-crease Paperfolding work of David Huffman, has since developed several ways to teach and work with curved folds and continues to investigate this underexplored topic in geometry. His inter- and cross-disciplinary work is situated at the intersection of computational geometry, digital manufacturing and material investigation. He likes to build proof-of-concept projects with students that investigate the scalability of ideas in geometry and computation. He has held several research positions at the Massachusetts Institute of Technology and has evaluated and documented all of Heinz Isler's models for the Heinz Isler Archiv at the Eidgenössische Technische Hochschule in Zurich in 2011.

Riccardo Foschi Tenure-Track Assistant Professor at the Department of Architecture, Alma Mater Studiorum University of Bologna. Ph.D. in architectural representation with a thesis on the algorithmic modelling of origami applied to architecture and manufacturing. His research interests are in the fields of representation and survey of architecture and product design, which span computational modelling, applied origami, digitization of artistic heritage, and virtual hypothetical reconstruction of unbuilt or lost heritage. He participated in funded projects aimed at standardizing the process of reconstruction of lost architectural heritage, and participates in the international research group "Structural Origami Gatherings". He is the author of numerous articles and has contributed to the organization of workshops, museum exhibitions, and events in his fields of expertise.

Rupert Maleczek an architect, researcher, and digital consultant, currently serving as a post-doctoral senior scientist at the Institute of Structure and Design (i.sd) within the Faculty of Architecture at the University of Innsbruck. He received his doctoral title in 2014 with his thesis on linear folded stripes, and has

since taught and collaborated with institutions and professionals worldwide. Maleczek's multidisciplinary work explores the intersections of geometry, form, structure, performance, materiality, and both digital and physical production. His research often focuses on the scalability of physical, geometrical, and biological phenomena, aiming to deepen the understanding of complex relationships and enhance their manageability through controlled simplification. Known as "simplexity," this approach makes sophisticated complex processes accessible to non-specialists. Additionally, he is the co-founder of the Structural Origami Group, an informal research network that investigates innovative approaches to Origami related structure and design.